Corner Bonding of CSPs: Processing and Reliability

Guoyun Tian, Yueli Liu, R. Wayne Johnson,
Pradeep Lall, Mike Palmer, & Nokib Islam
Laboratory for Electronics Assembly &
Packaging – Auburn University
162 Broun Hall, ECE Dept.
Auburn, AL 36849 USA
334-844-1880
johnson@eng.auburn.edu

Larry Crane
Henkel Loctite Corporation
Loctite Electronic Materials
Industry, CA
800-827-2207 x401
Larry_Crane@loctite.com

ABSTRACT

The use of CSPs has expanded rapidly, particularly in portable electronic products. Many CSP designs will meet the thermal cycle or thermal shock requirements for these applications. However, mechanical shock (drop) and bending requirements often necessitate the use of underfills to increase the mechanical strength of the CSP-to-board connection. Capillary flow underfills processed after reflow, provide the most common solution to improving mechanical reliability. However, capillary underfill adds board dehydration, underfill dispense, flow and cure steps and the associated equipment to the assembly process.

Corner bonding provides an alternate approach. Dots of underfill are dispensed at the four corners of the CSP site after solder paste print, but before CSP placement. During reflow the underfill cures, providing mechanical coupling between the CSP and the board at the corners of the CSP. Since only small areas of underfill are used, board dehydration is not required.

This paper examines the manufacturing process for corner bonding including dispense volume, CSP placement and reflow. Drop test results are then presented. A conventional, capillary process was used for comparison of drop test results. Test results with corner bonding were intermediate between complete capillary underfill and non-underfilled CSPs. Finite element modeling results for the drop test are also included.

INTRODUCTION

While portable products are reaching sizes limited by human-machine interfaces (keypads, displays, etc.) the push to increased feature content continues to drive the electronics packaging and manufacturing industry to ever smaller packages. Portable products have driven the dramatic growth in the use of chip scale packages (CSPs) with one or more semiconductor die inside. Compared to flip chip on laminate (FCOL), CSPs provide pre-testability which is critical in high volume, low cost applications.

Many CSPs have been developed to provide the necessary thermal cycle/thermal shock reliability for portable product applications. However, with decreasing pad sizes and solder joint volumes, field failures due to dropping of the product occur. Two solutions are possible. Improved mechanical design of the product to minimize shock and board flexing when the product is dropped is one approach. However, with very short product life cycles and correspondingly short design cycles, this is often not possible. The second approach is to use underfill to 'reinforce' the CSP, by bonding it to the PWB [1-3]. This approach does not impact design time, but does increase unit manufacturing costs. Today, underfilling CSPs is common practice.

Capillary underfill is most commonly used with CSPs. After reflow assembly, the underfill is dispensed along one or two edges of the CSP. Capillary forces pull the underfill under the CSP, filling the gap between the CSP and the printed circuit board (PCB). The underfill is then cured. If moisture is present in the PCB, a dehydration bake is required prior to underfilling to eliminate voids in the underfill. [4]. Reworkable capillary underfills are available if the option of rework after underfilling is required [2, 4].

A second option for CSP underfill is fluxing or no-flow underfills. In this process, fluxing underfill is dispensed at the CSP site prior to CSP placement. No solder paste is printed at the site. The CSP is placed and reflowed in a standard reflow cycle. This process eliminates the flow and cure times, but requires a dehydration bake to remove moisture from the board. Without dehydration, the moisture will be liberated during the reflow cycle, creating voids in the underfill that may degrade reliability. It is also important that the solder mask be fully cured and not evolve solvents during reflow. The placement parameters and reflow

profile must be optimized to reduce underfill voiding, achieve good solder wetting and ensure a complete cure of the underfill [4]. Fluxing underfills are not reworkable.

The approach explored in this work is referred to as 'corner bonding'. In this approach a specially formulated (high viscosity) underfill is dispensed at the four corners of the CSP site after solder paste printing, just prior to CSP placement. The CSP is then placed and reflowed. During the reflow cycle the underfill cures, providing reinforcement at the four corners of the CSP. Since the underfill dots are relatively small, a dehydration bake is not required. With a smaller contact area compared to full capillary underfill, the assembled CSPs can be removed using a standard hot air rework station. The assembly and rework processes are discussed in the next sections.

TEST VEHICLE

The test vehicle was a four-layer test board with 10 CSP attachment sites per side. The board was designed for a 12mm CSP on one side and an 8mm CSP on the other. In this work, only the 8mm CSP was used. Standard technology was used for board fabrication, no build-up or HDI layers. The board was 2.95" by 7.24" by 0.042" thick. Drill holes (0.013" drill) under the 12mm CSP were plugged and tented to prevent underfill from flowing through the hole during dispense. The pads were 0.010" in diameter, non-solder mask defined with an electroless nickel/immersion gold finish. Initial drop testing experiments yielded inconsistent results. Failure analysis revealed failure at the interface between the nickel and the intermetallic layer (Figure 1). This is indicative of black pad associated with electroless nickel/immersion gold [5]. Boards were obtained from a second supplier with an immersion silver finish and used for the remaining experiments.

The CSP was an 8mm, 0.5mm pitch, 132 I/O TapeArray manufactured by Amkor Technology and purchased from Practical Components (A-TArray132-.5mm-8mm-DC). The I/O were on a 14 x 14 array with only the outer three rows populated. The CSP was a daisy chain test part for continuity measurements. The silicon die was 3.98mm x 3.98mm.

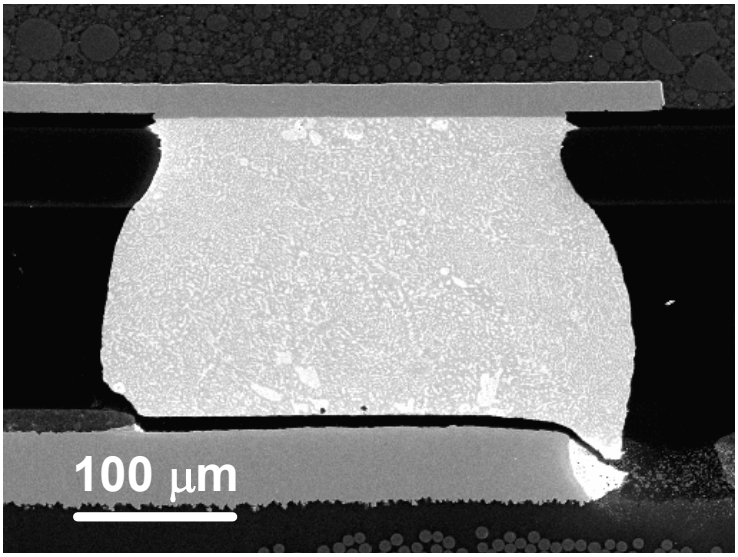

(a)

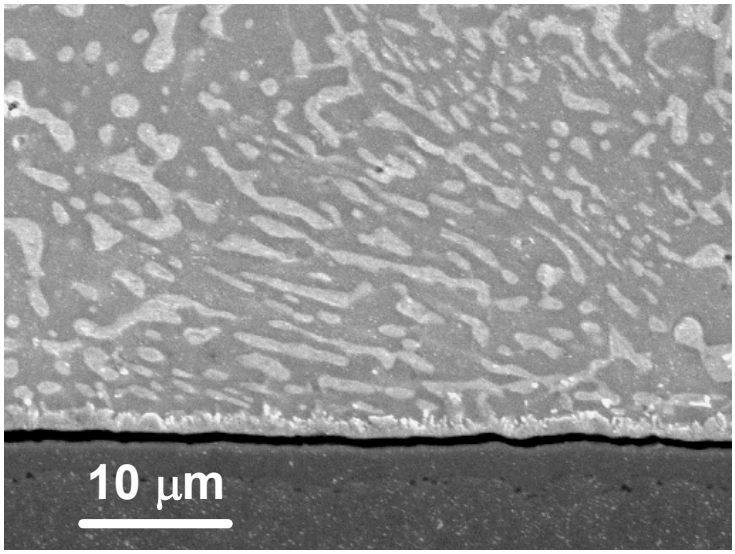

(b)

Figure 1. Cross Section (a) and Close-up (b) of Failed Solder Joint after Drop Test Using Printed Wiring Board with Electroless Ni/Immersion Au Finish.

ASSEMBLY

The test vehicles were assembled on an automated SMT line at Auburn University. No-clean solder paste was printed with an MPM AP25 stencil printer using a 4 mil thick, laser cut, electro-polished, nickel plated stencil. The solder paste print was then inspected. For those CSPs assembled with corner bond underfill (Loctite 3515), the underfill was dispensed with a Camalot 3700 dispense system after solder paste print. Four dots were dispensed at the four corners of the CSP site (Figure 2). No board heat was used. The dot was positioned so that the corner of the CSP was in the center of the dispensed dot (Figure 3). Dispense experiments were performed to optimize the dispense process. The dispense system used a rotary valve dispense head. Since the viscosity of the underfill was higher than traditional capillary flow underfills, the effect of fluid pressure on dot volume consistency was measured using the volumetric measuring system on the dispense system. The dispense time was varied to maintain the same volume at the two fluid pressures. The results are shown in Table 1. The coefficient of variation (CV) was lower at the higher fluid pressure and the difference between minimum and maximum volume was less. For the test vehicle assembly, each dot was dispensed with a pressure of $1.2x10^5 N/m^2$ and a volume of 0.64μl.

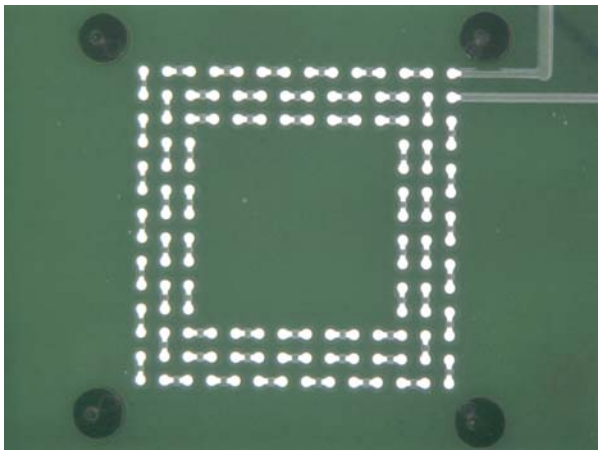

Figure 2. Corner Dot Dispense Pattern.

Figure 3. CSP Placed into Corner Dot Underfill.

Table 1. Results of Dispense Volume Uniformity versus Fluid Pressure Experiments

Fluid Pressure	$0.6x10^5 N/m^2$	$1.2x10^5 N/m^2$
Average Volume (μL)	0.6353	0.640
Std. Dev. (μL)	0.031	0.007
Max (μL)	0.668	0.654
Min (μL)	0.535	0.628
CV (%)	4.80	1.10

The CSPs were placed with a Siemens F5 machine using a placement force of nine Newtons. The boards were then reflowed in a Heller 1800 EXL furnace in air. Two profiles were evaluated. Figure 4 shows a conventional profile with a soak prior to reflow. For low mass, high volume portable product boards, ramp profiles (Figure 5) are more common to reduce the total time in the furnace, increasing throughput.

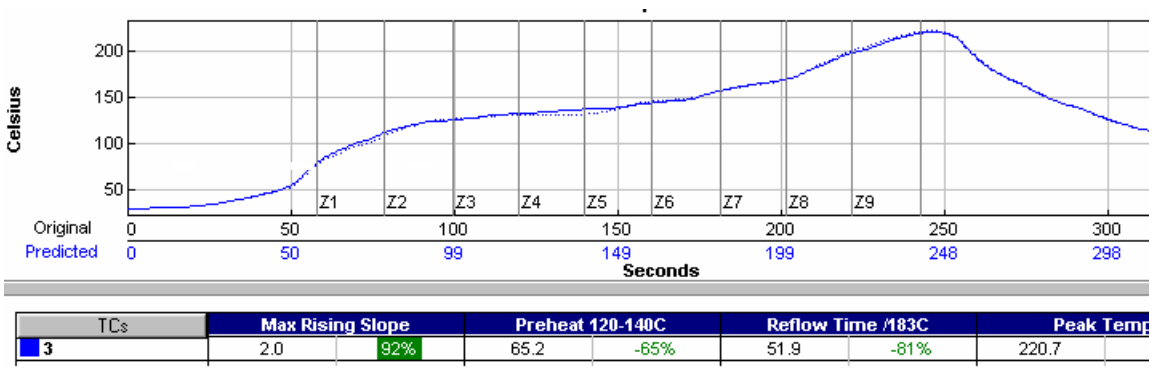

Figure 4. Conventional Soak Reflow Profile.

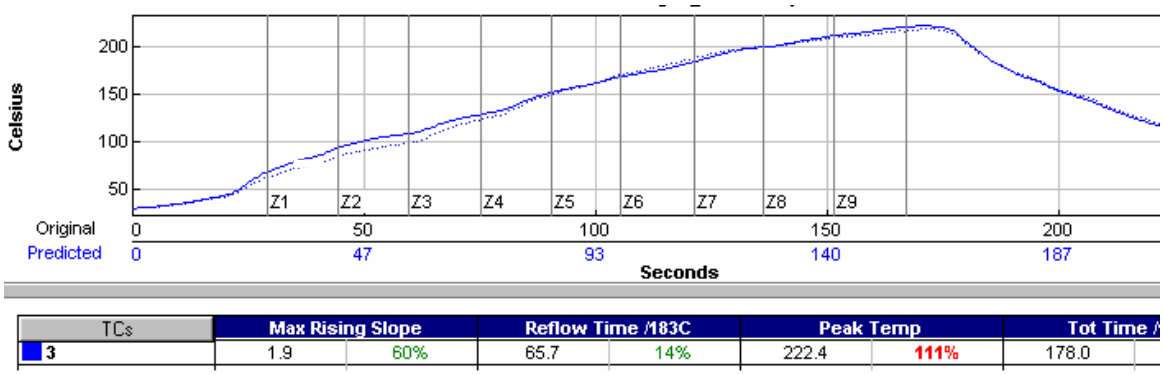

Figure 5. Ramp Reflow Profile.

Differential scanning calorimetry (DSC) was used to evaluate the underfill cure with the two profiles. For comparison, a sample was cured for 45 minutes at 150°C in a box oven. A DSC plot of an uncured sample is also plotted. As shown in Figure 6, there is no exotherm associated with either reflow profile, indicating a high degree of cure. Figures 7 and 8 show cross sections of solder joints for both profiles and indicate good wetting and collapse (the underfill does not become too viscous before the solder collapses). For the subsequent experimental work, the ramp profile was used.

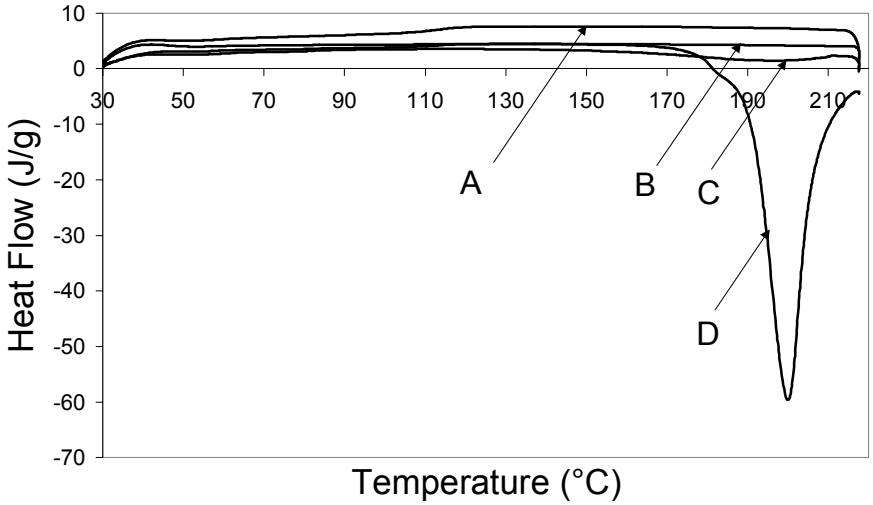

Figure 6. DSC of Loctite 3515 (A– Soak, , B – Ramp, C – Box Oven, D – Uncured); (Heating rate = 20°C/min., Purge gas = Nitrogen (50 ml/min). Instrument Model - TA Instruments DSC2920 Modulated DSC.

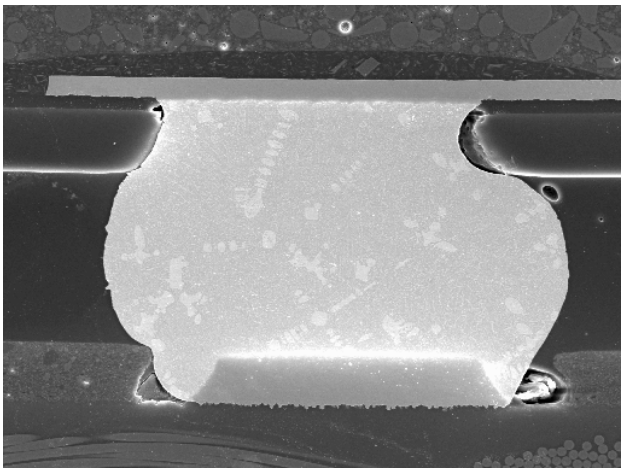

Figure 7. Cross Section of Solder Joint Showing Excellent Wetting with Soak Profile.

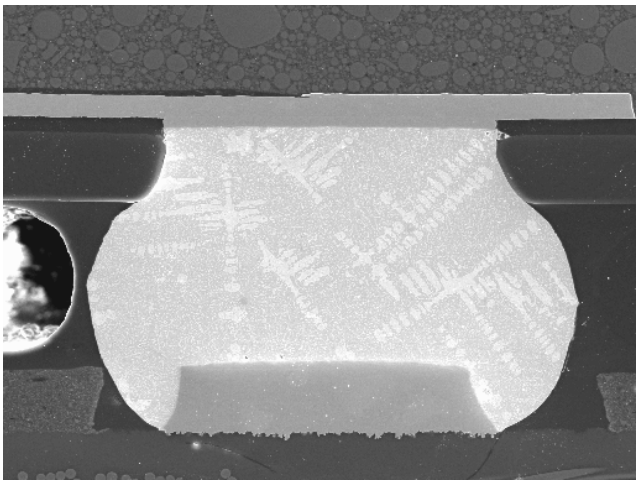

Figure 8. Cross Section of Solder Joint Showing Excellent Wetting with Ramp Profile.

Figure 9 shows an x-ray image of a CSP intentionally placed 5 mils off center (50% mis-alignment). After reflow, the CSP has self-centered (Figure 10) indicating no influence of the underfill dots on self-centering.

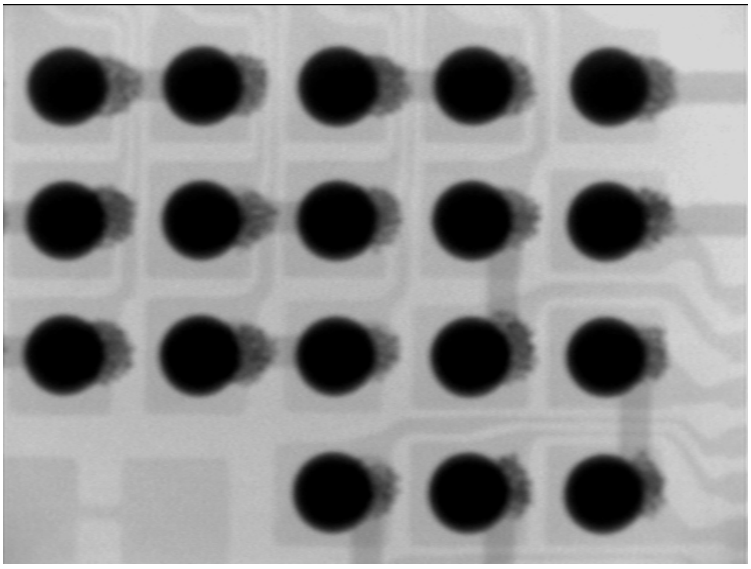

Figure 9. X-ray Image of a CSP Intentionally Placed with a 5 mil (50%) Offset.

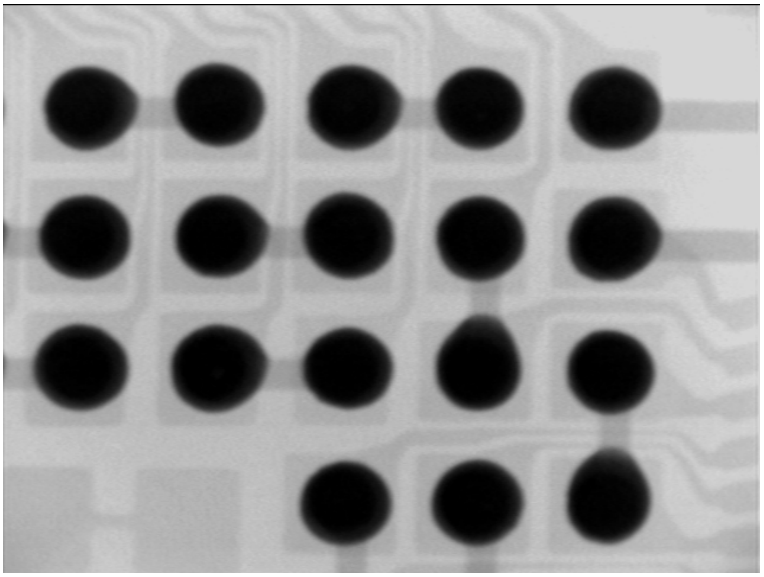

Figure 10. X-ray of CSP after Reflow.

For comparison, CSPS with no underfill and with capillary flow underfill (Loctite 3593) were also built using the ramp reflow profile. For the capillary flow underfill, the boards were dehydrated at 125^{o}C for fifteen hours prior to underfill dispense. The dehydration bake was necessary to remove moisture absorbed by the board during the time between reflow and the underfill dispense [4]. An 'L' shaped dispense pattern was used. The underfill was cured in a box oven at 165^{o}C for five minutes. Samples were flat sectioned to verify a complete underfill with no voids. As has been previously shown, there were pockets of trapped flux residue around the base of the solder balls [1, 4].

REWORK

To evaluate the mechanical strength of the corner dot adhesive, dots were dispensed and cured through a reflow cycle without a CSP placed. Using a Dage PC 2400 shear tester with a heated stage, the dots were sheared at different substrate temperatures and the shear force was recorded. The results are plotted in Figure 11. As can be seen the mechanical strength drops rapidly at the 175^{o}C. This allows removal of the

CSP for rework. Using an Air-Vac DRS 24C rework station, CSPs were removed at a temperature of 220°C using a modified nozzle that allowed a small amount of torque to be applied to the CSP to shear the underfill.

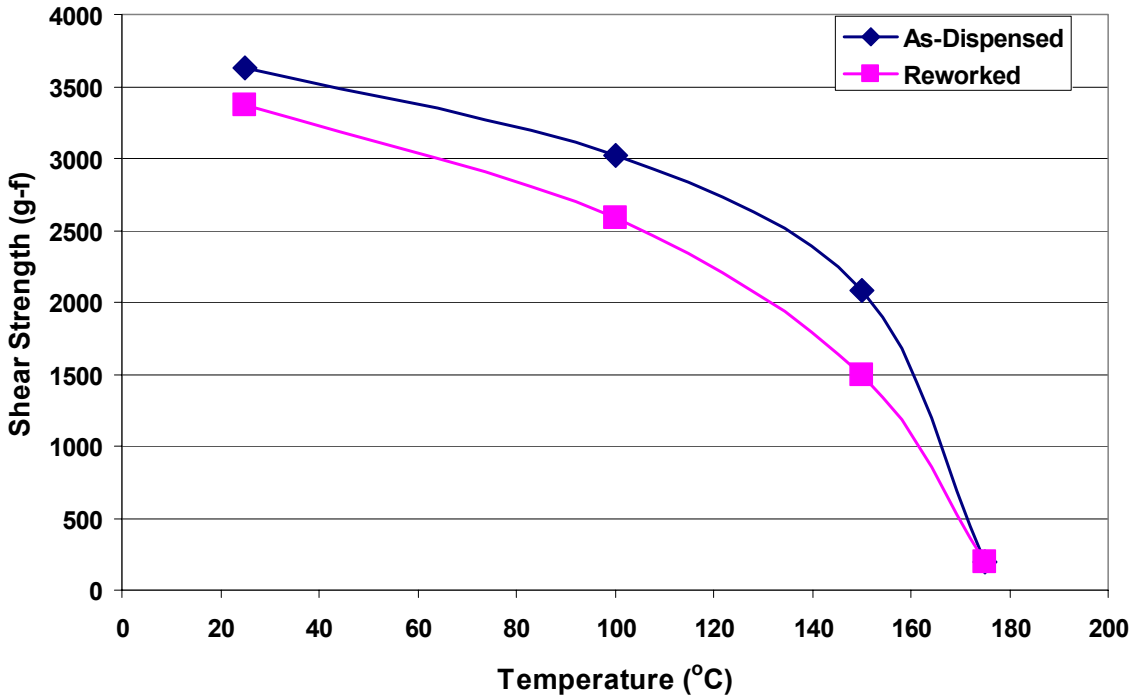

Figure 11. Adhesive Dot Shear Strength as a function of Temperature

As shown in Figure 12, the CSP can be removed with no damage to the board. There is corner bond underfill residue remaining. Using the dressing tool on the rework station, most of the underfill can be removed (Figure 13). It is not necessary to remove the entire residue, since there is no degradation of the underfill residue during rework. To verify this, underfill dots were dispensed and reflow cured. Then the bulk of the dot was removed using the rework station dressing tool. A second underfill dot was dispensed over the residue and reflow cured. The second dot was shear tested with a Dage 2400 shear tester as a function of temperature (Figure 11). The average shear strength of the 'reworked' dot was nearly the same as the original dot. The difference in shear strenght is likely due to a slightly smaller contact area for the second dot dispense. In all cases, the room temperature failure mode was cohesive failure in the PCB laminate – chunks of laminate were pulled out, exposing the glass fiber bundles.

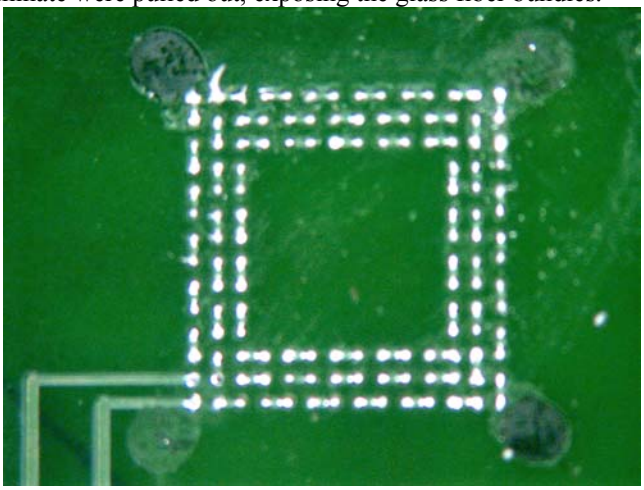

Figure 12. CSP Site after CSP Removal.

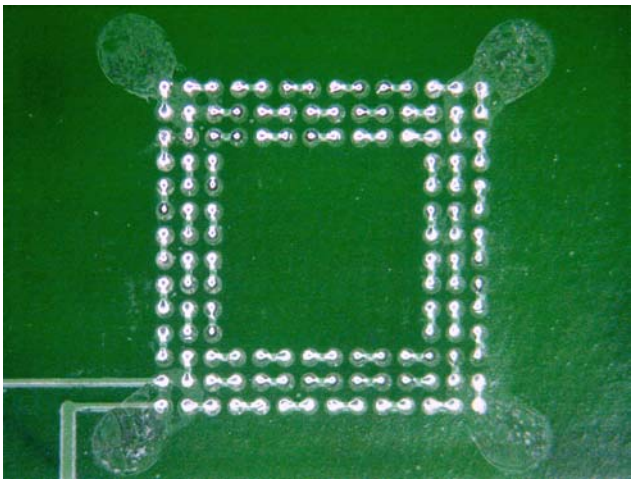

Figure 13. CSP Site after Dressing.

For reassembly, a flux dip, underfill dispense, place and reflow process was used. The drop test and liquid-to-liquid thermal shock performance of flux-only assembly has been shown comparable to using solder paste and is suitable for repair [5].

DROP TEST RESULTS

For mechanical shock testing, a 31.8 gram weight was attached to one end of the board as shown in Figure 14 to accelerate failure and simulate product weight. The board (weighted end up) was then dropped through a six foot long, three inch diameter tube onto a concrete floor. The daisy chain resistance of each CSP was measured and a 10% increase in resistance was recorded as a failure. Four boards (40 CSPs) were tested and the results are shown in Figure 15. As can be seen in the plot, capillary underfill provides the most reliable assembly, with the corner dots providing approximately a 3-4x improvement compared to no underfill.

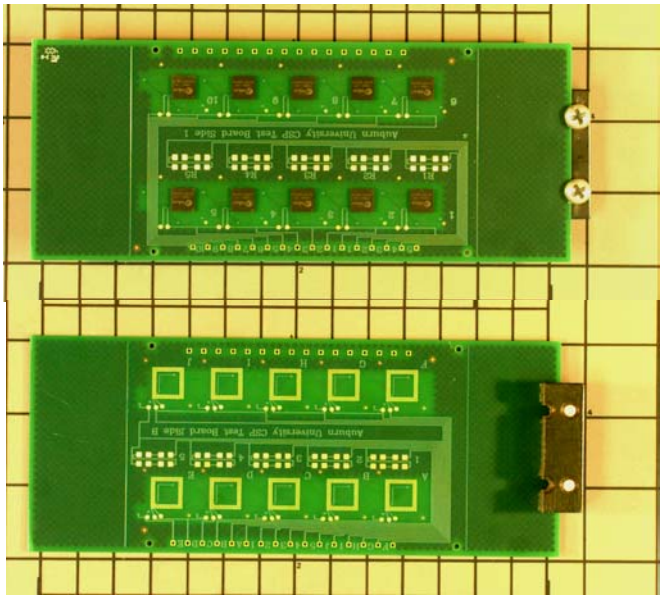

Figure 14. Photographs of Test Board (front and back) with Weight (31.8g) Attached to Backside (non-CSP side) for Drop Test.

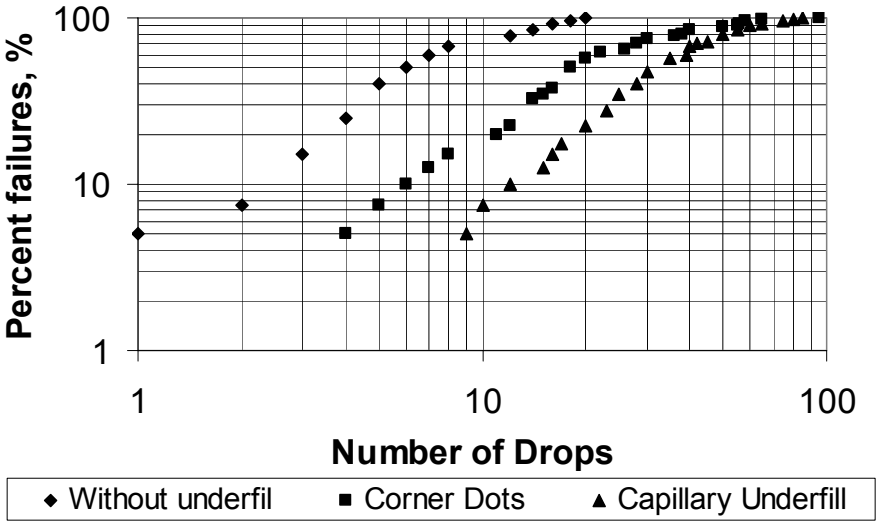

Figure 15. Drop Test Results.

Failure Analysis

No Underfill: Cross sections were made of failed CSPs after drop testing. Figure 16 shows failure in the solder on the package side with no underfill.

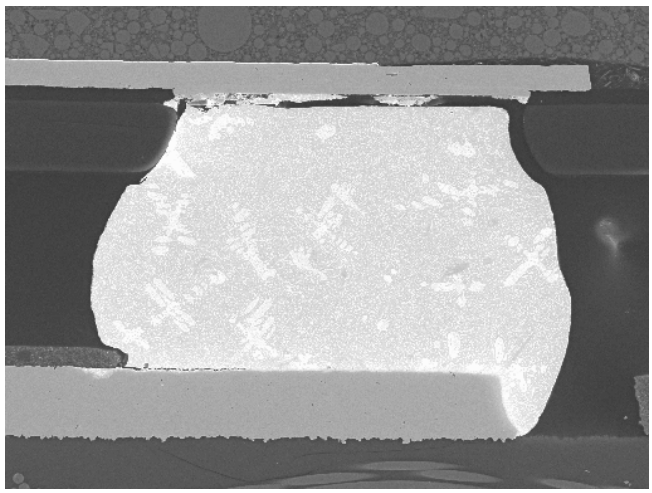

Figure 16. Cross Section of Failed Solder Joint (No Underfill).

Figure 17 shows cracking in the printed circuit board under the solder pad. In some case, the entire CSP came off the board by cohesive failure in the laminate material. The copper pads and chunks of laminate were removed, leaving exposed glass fiber bundles. In some cases, the part had been electrically good on the drop just before the drop in which the CSP came off the board, thus a massive failure.

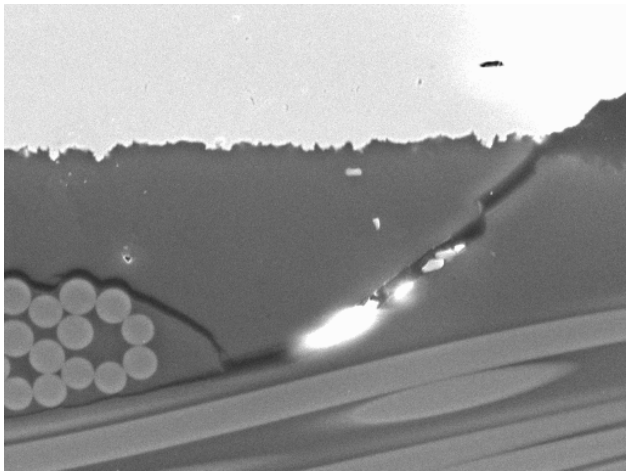

Figure 17. Crack in Laminate under Solder Pad (No Underfill).

Corner Bond: Figure 18 shows cracking of the corner bond underfill after drop testing. At the end of the drop test (total of 80 drops) there was cracking of at least one dot of the corner bond material on each CSP. Figure 19 shows cracking of the copper and laminate after drop testing. Although not as common, some CSPs from corner bonded samples came completely off the board during drop testing. In most case, electrical failure had already occurred.

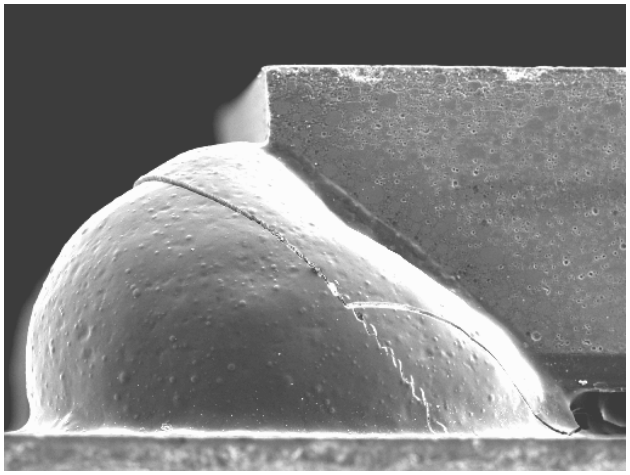

Figure 18. Photograph of Cracked Corner Bond Underfill after Drop Testing.

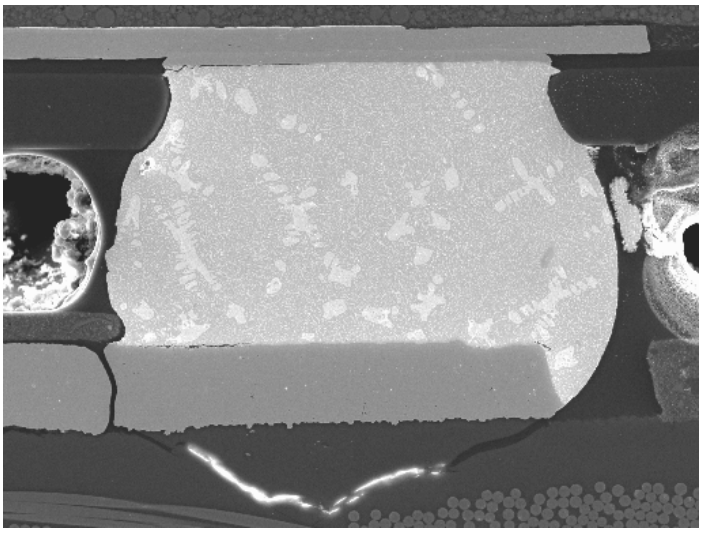

Figure 19. Cracking of Copper and Laminate after Drop Testing. Sample was Corner Bonded.

Figure 20 shows a failure with the capillary underfill. A crack propagates from the underfill fillet, along the solder mask-copper interface, then through the copper trace and into the laminate. In this case, the capillary underfilled CSP creates a very rigid area on the otherwise relatively flexible PCB. During the PCB flexing that occurs immediately after impact, the transition region from flexible-to-rigid areas is most susceptible to cracking. Again, there were a few instances in which the CSP came off the board during the drop test (100 total drops per board).

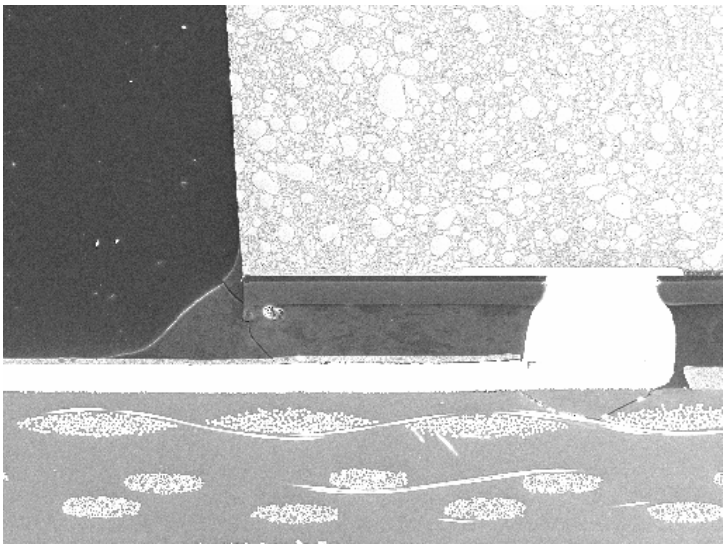

(a)

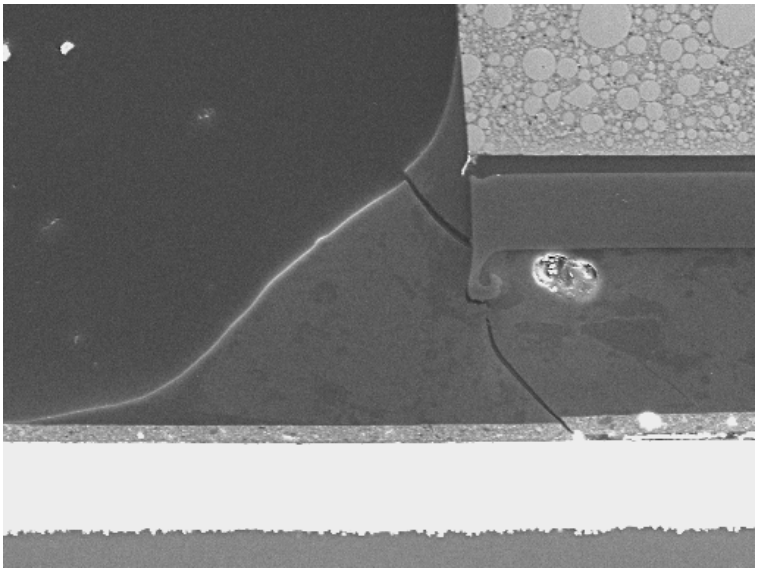

(b)

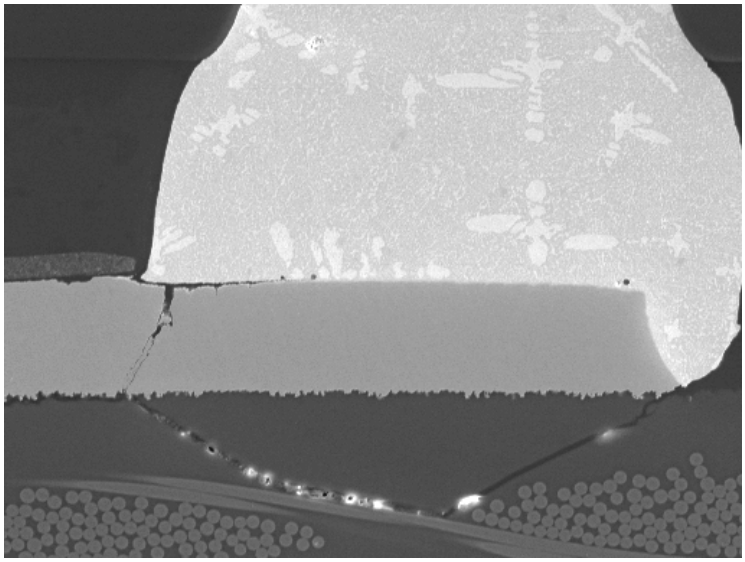

(c)

Figure 20. Cross Section of Crack in Capillary Underfilled CSP after Drop Test (a – low magnification). (b) Close-up of Crack in Underfill Fillet. (c) Close-up of Crack in Copper and Laminate.

EXPLICIT FINITE-ELEMENT MODEL

Transient dynamic behavior of a populated printed circuit board during drop from 6ft. has been simulated using explicit time-integration in ABAQUS Explicit. An initial velocity of 5.99 m/s has been assigned to the board, components and the weight at the top edge of the board. The board has been modeled with shell S4R elements and the components have been modeled with solid C3D8R elements. Smeared stiffness properties have been derived for the components. The approach used for smeared properties in this paper follows the approach proposed by Clech [6, 7] for development of closed form models for solder joints subjected to thermal fatigue. The equation is:

$$\upsilon_C = \frac{\sum_{k=1}^{n} \upsilon_k h_k}{\sum_{k=1}^{n} h_k} \qquad \frac{E_C h_C^3}{12(1-\upsilon_C)} = \sum_{k=1}^{n} \frac{E_k h_k^3}{12(1-\upsilon_k)}$$

where E is the elastic modulus, ν is the Poisson's ratio, h is the layer thickness. Subscript "C" indicates smeared material and subscript k indicates individual materials. The concrete floor has been modeled with rigid R3D4 elements. A reference node has been placed behind the rigid wall for application of constraints. Contact has been monitored between any PCB surface, CSP surface or Weight surface and only on the positive side of the floor. Node to surface contact has been used. An event length of 30 ms after impact has been modeled. Time history has been monitored at a time period of 0.1 ms at the corner of all CSPs.

Experimental transient response of the board has been measured using a high-speed camera at 38,000 frames per second. Figure 21 shows the correlation between the model predictions and high-speed video at 4.5 ms, 7.5 ms and 18 ms after impact. The transient mode shape of the board from model prediction shows good correlation with experimental data.

Comparisons between various energy components has been used to help evaluate whether an analysis is yielding an appropriate response. One may not know ahead of time which parts of the model are likely to become unstable. Kinetic energy for each increment has been used to provide a simple indication of stability. Kinetic energy is summed over the entire model and therefore provides a superior means of evaluating stability compared to monitoring a particular degree of freedom. While, the unrealistic growth in the kinetic energy may indicate that the analysis has become unstable, it does not indicate the problem area. Figure 22 shows the energy balance in the model over the 30 ms simulated drop event. Notice how the kinetic energy (ALLKE) dissipates after impact. Further, the sum of various energy components (ETOTAL, Figure 22), should be constant. In the numerical model presented, the total energy is approximately constant, with an error of less than 1%.

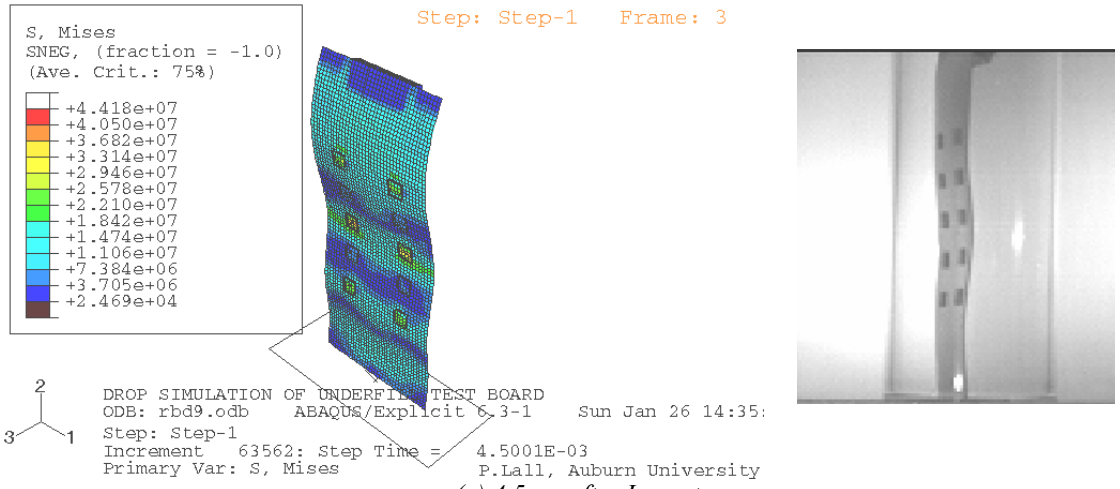

(a) 4.5 ms after Impact

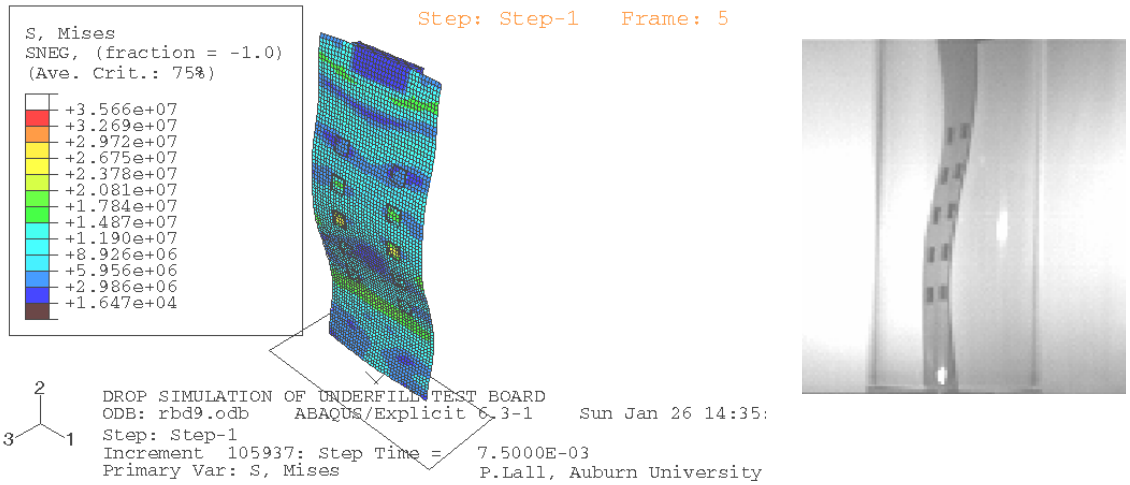

(b) 7.5 ms after Impact

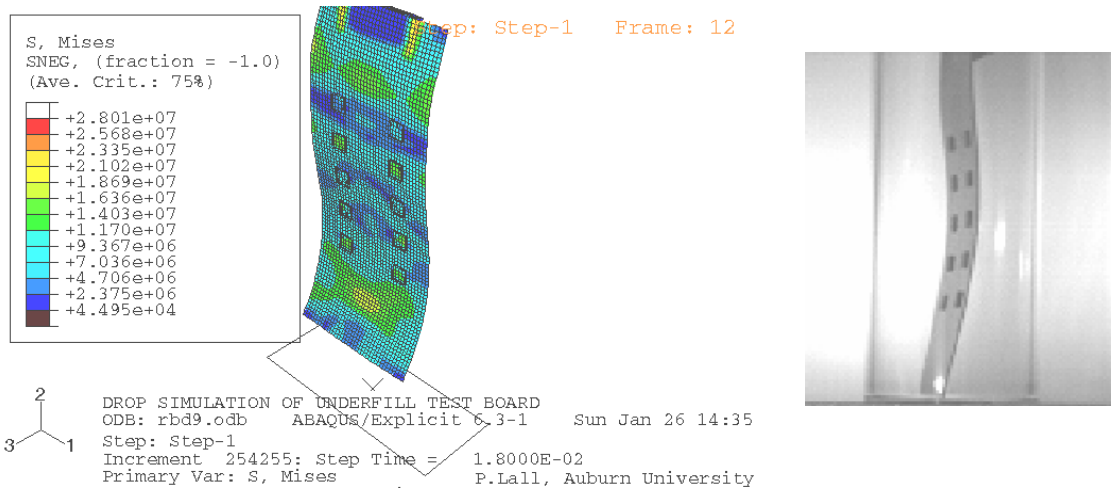

(c) 18 ms after Impact

Figure 21. Model Predictions and High-Speed Video (38,000 fps) of Board Deformation during a 6-feet drop.

The global coordinate system has been defined as direction-1 along PCB width, direction-2 along PCB length, and direction-3 along PCB thickness. There are five rows and two columns of CSPs on the printed-circuit board. The rows and columns are numbered from top down and left to right. The top left corner being (row 1, column 1). In the interest of database size, only three rows of chip locations have been monitored in time history data. The top row, middle row, and the bottom row. A sign convention of "ijLEmk" has been adopted in Figures 23-24 where "i" is the row number, "j" is the column number for the CSP location on the board, LE signifies logarithmic strain, "m" signifies the face, and "k" signifies the direction on which the strain is measured. Thus, "11LE22" indicates the logarithmic strain ε_{22} at the CSP corner in location row 1, and column 1. Figure 23 indicates that the strains are primarily in direction-2, along the length of the PCB. The overlapping strain values at 11LE22, and 12LE22 indicate that there is almost no twisting of the PCB during drop (Figure 24).

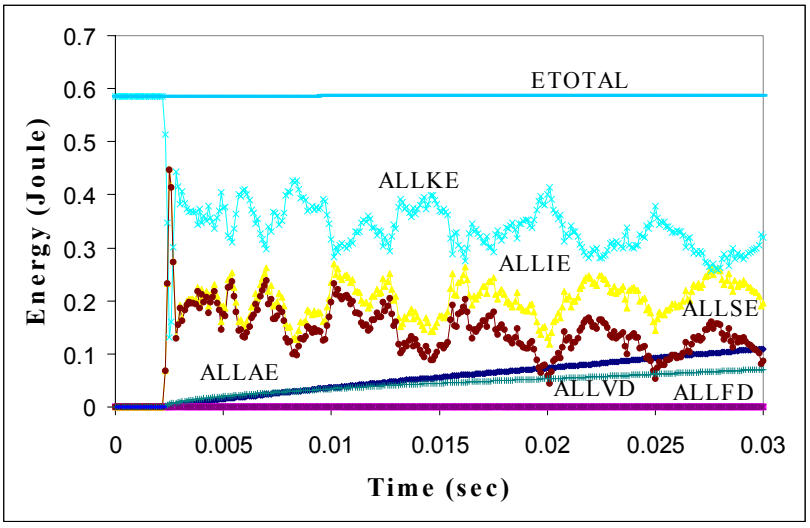

Figure 22. Model Energy Balance.

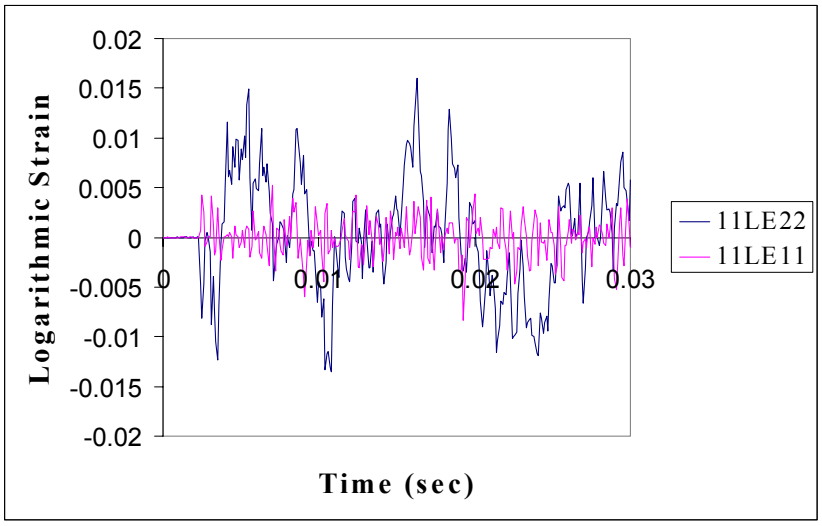

Figure 23.Logarithmic Strains LE11, LE22 at Location 11 CSP Corner.

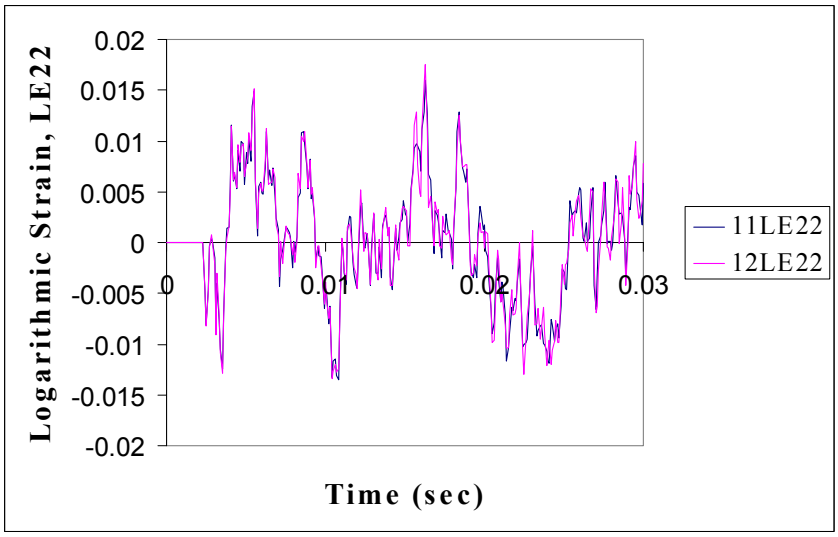

Figure 24: Logarithmic Strains LE22 at Location 11 and 12 CSP Corner.

A local model of the CSP has been developed to evaluate the solder joint reliability. Figure 25 shows a slice-model of the chip-scale package with corner bonded underfill. The solder behavior has been modeled with non-linear Anand's Viscoplasticity in ANSYS. VISCO107 elements have been used for solder and SOLID45 for package and board elements. The approach used for model development is discussed in detail in [8].

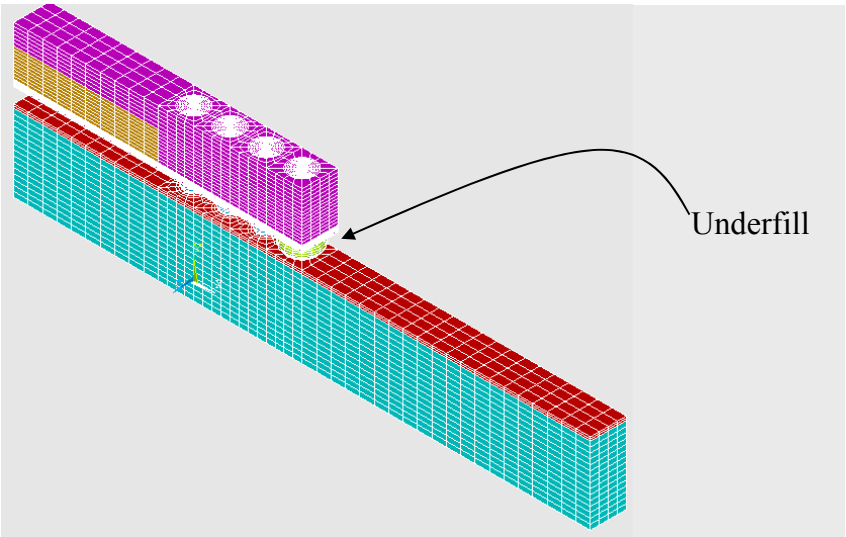

Figure 25. Local model of CSP with Corner-Bond Underfill.

Figure 26 shows the plastic work in the corner solder joint versus deformation of the center of the package with respect to the board location at 2x package lengths from the center of the package. The plastic work reported is an average of the plastic work for corner elements.

Model predictions indicate that there is up to a 52% reduction in the plastic work for corner solder joints due to the presence of corner underfill in the package. It is therefore expected that the CSP with corner bond will have a better resistance to damage during product drop.

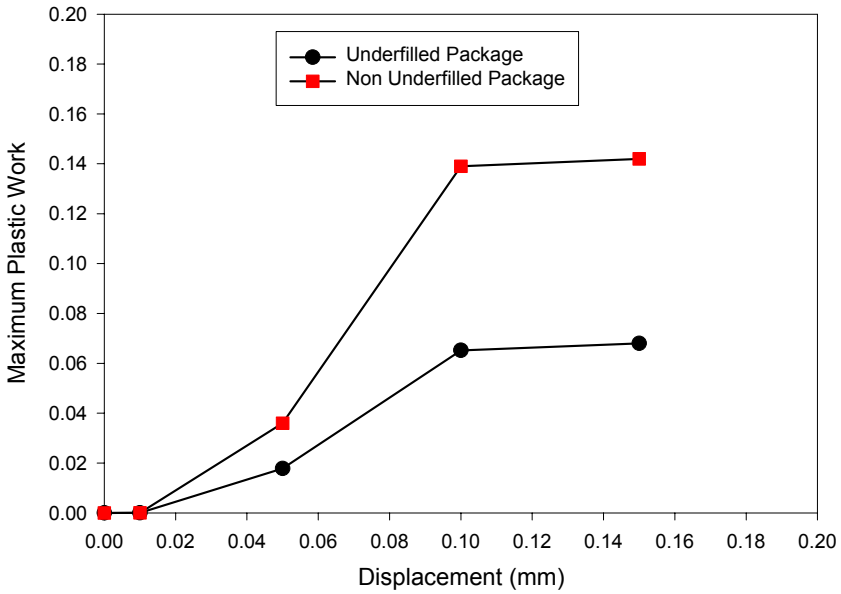

Figure 26. Effect of corner-bonded underfill on the plastic work in the solder joint.

Summary

Corner bonded underfill provides a simplified manufacturing process for CSPs that require underfill, eliminating the dehydration bake, capillary flow time and cure. While the drop test reliability is not as high as with complete, capillary underfill, corner bond underfill provides a 3-4x improvement compared to no underfill. Corner bond underfill is a viable, cost-effective approach for many portable product applications.

References

1. Haiwei Peng, R. Wayne Johnson, George Flowers, Erin Yeager, Mark Konarski, Afranio Torres, and Larry Crane, “Underfilling Micro-BGAs,” Proceedings of the International Conference on High-Density Interconnect and Systems Packaging, Denver CO, April 25-28, 2000, pp. 134-140.
2. Nael Hannan, Puligandla Viswanadham, Larry Crane, Erin Yaeger, Afranio Torres, and R. Wayne Johnson, “Reworkable Underfill Materials For Improved Manufacturability And Reliability Of CSP Assemblies,” Proceedings of the 2001 APEX Conference, San Diego, CA, January 14-18, 2001, pp. AT8-3-1 – AT8-3-10.
3. Steven J. Young, “Underfilling BGA and CSP for Harsh Environment Deployment,” Proceedings of the 1999 International Conference on High Density Packaging and MCMs, Denver, CO, April 7-9, 1999.
4. Jing Liu, R. Wayne Johnson, Erin Yaeger, Mark Konarski and Larry Crane, “CSP Underfill, Processing and Reliability,” Proceedings of the 2002 APEX Technical Program, January 19-24, 2002, San Diego, CA, pp. S16-1-1 to S16-1-7.
5. Bruce Houghton, “Solving the ENIG Black Pad Problem: An ITRI Report on Round 2,” Proceedings of IPC Works ’99, Oct. 23-28, 1999, Minneapolis, MN, pp. S-04-3-1 to S-04-3-9.
6. J-P. Clech., “Solder Reliability Solutions: a PC-based Design-for-reliability Tool,” Proceedings of the Surface Mount International Conference, Sept. 8-12, San Jose, CA, Vol. I, pp. 136-151, 1996.
7. J-P. Clech, "Flip-chip/CSP Assembly Reliability and Solder Volume Effects", Proceedings of the Surface Mount International Conference, San Jose, CA, August 25-27, 1998, pp. 315-324.
8. P. Lall, and K. Banerji, “Assembly-Level Reliability of Flex-Substrate BGA, Elastomer-on-Flex Packages, and 0.5 mm Pitch Partial Array Packages,” Microelectronics Reliability Journal, Vol. 40, pp. 1081-1095, 2000